Amin et al., https://doi.org/10.1085/jgp.201711762

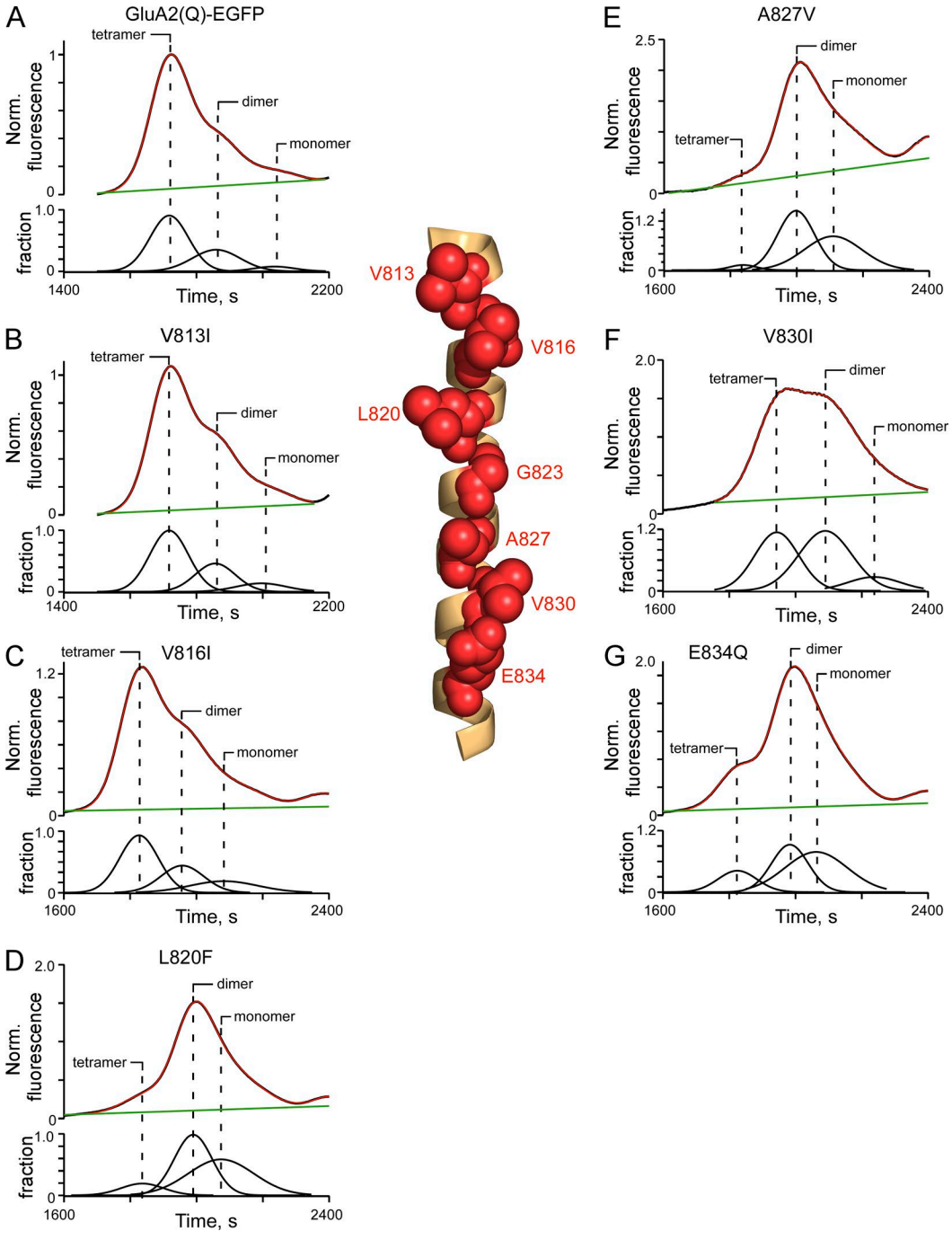

Figure S1. **Example FSEC chromatographs for substitutions of the VVLGAVE face of the GluA2 M4 segment (relates to Fig. 2).** (A–G) FSEC chromatographs of wild-type GluA2(Q)-EGFP (A) and "subtle" substitutions in the VVLGAVE face (B–G). As example substitutions, we generally selected side chains that were slightly larger in volume than the native side chain while largely maintaining its general chemical properties (Table S1). Example records are displayed and analyzed as in Fig. 2. (middle) Structure of the GluA2 M4 segment with the various positions in the VVLGAVE face highlighted in red. Note the location of the various peaks (tetramer, dimer, and monomer) varied between different transfection cycles/FSEC runs (e.g., compare wild-type GluA2(Q)-EGFP shown here [A] and in Fig. 2 A) but within runs was consistent (A and B here and Fig. 2 [A and B] were obtained during same transfection cycle/FSEC run).

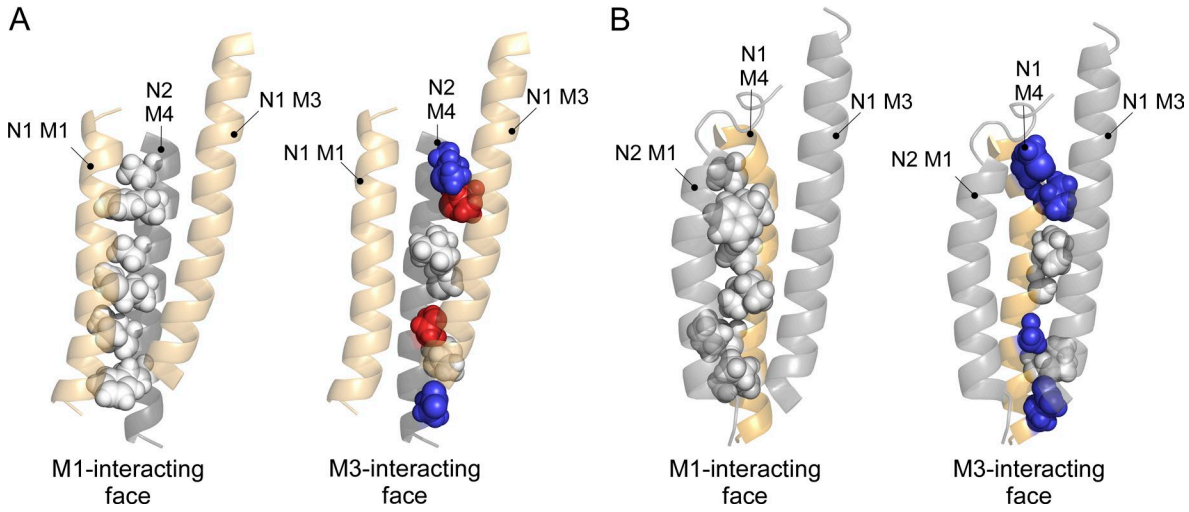

Figure S2. **Structural analysis of M1- and M3-interacting faces of the M4 segments in GluN1 or GluN2B (relates to Fig. 3).** (A) Comparison of GluN2B M4 segment interacting faces, either M1-interacting face (left, side chain positions A818, F821, A825, M828, L832, and F835) or M3-interacting face (right, side chain positions M817, V820, L824, A827, S831, T834, and E838). Side chains are colored based on current amplitudes in tryptophan scan (Fig. 3 and Table S2): light gray, not significantly different from wild type; blue, significantly reduced; and red, no detectable current. (B) Comparison of GluN1 M4 segment interacting faces, either M1-interacting face (left, side chain positions A814, F817, A821, I824, I828, and I831) or M3-interacting face (right, side chain positions M813, V816, V820, G823, G827, L830, and E843). M4 side chain coloring as in A. GluN1 helices are colored light orange, and GluN2B helices are colored gray 60%. View of the M4 is positioned in between the M1 and M3 helices (ghosted) to give perspective on potential structural interactions. Note significant changes in whole-cell current amplitudes only occurred for those positions that interact with the M3 segments.

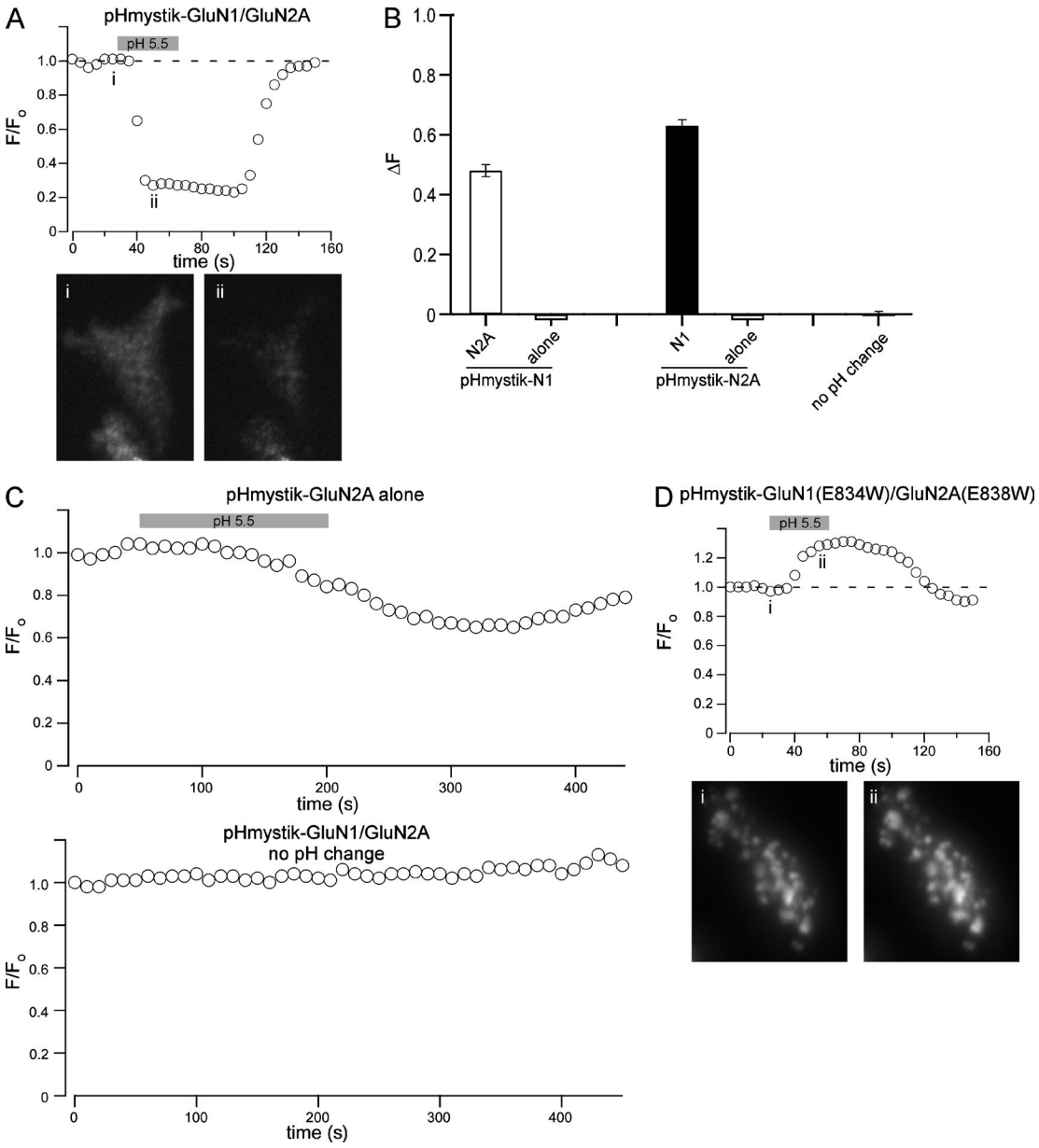

Figure S3. **Characterization of NMDAR subunits containing pHmystik (relates to Fig. 4).** (A) Fluorescence time trace of GFP intensity as the extracellular bath solution pH was changed from 7.4 to 5.5 (gray bar, 30-s duration) and back again for pHmystick-GluN1/GluN2A. The representative images below the panel show the cell that was analyzed to generate the time trace; the images were taken at the approximate time points when the baseline fluorescence (F_o), corresponding to image i, and the test fluorescence (F_{test}), corresponding to image ii, were measured. The change in fluorescence ($\Delta F = F_o - F_{test}$) was used as an index of surface expression of NMDARs. Sampling rate, 5 s. (B) Mean changes (±SEM) in fluorescence for wild-type constructs or the corresponding subunit expressed alone or if no pH change was made (no pH change). In all instances, fluorescence changes (ΔF) were measured within 30–50 s of switching the external solution from pH 7.4 to 5.5. Number of cells recorded: pHmystik-GluN1/GluN2A (28), pHmystik-GluN1 alone (16), GluN1/pHmystik-GluN2A (17), pHmystik-GluN2A alone (8), and no pH change (8). (C) Representative example showing the effect of lengthened exposure to pH 5.5 (150-s application) on the fluorescence intensity for pHmystik-GluN2A alone. A similar response to long exposures also occurred for pHmystik-GluN1 expressed alone (not depicted). For this reason, we used only rapid changes in fluorescence intensity (e.g., panel A or Fig. 3 [A–C]) as an index of surface expression. Sampling rate, 10 s. (D) Example of an increase in fluorescence intensity during switch to pH 5.5. The images below are from the labeled time points, indicating that increases in fluorescence intensity occurred with previously present puncta rather than arising from new puncta. Such increases in fluorescence intensity were always associated with constructs that presumably do not express on the membrane (i.e., we could not detect measurable glutamate-active current). For pHmystik-GluN1(E834W)/GluN2A(E838W), such an increase occurred in 8 out of 20 cells. Sampling rate, 5 s.

Table S1. **Side chain properties of "subtle" substitutions in the VVLGAVE face of the GluA2 M4 segment (relates to Fig. 2)**

Position	Average volume	"Subtle" substitution	Average volume	Additional comments on side chain properties
	Å^3		*Å*^{3}	
Valine (V813)	141.7	Tryptophan (W)	237.6	
		Alanine (A)	91.5	
		Leucine (L)	167.9	
		Isoleucine (I)	168.8	like valine, branch-chained
Valine (V816)	141.7	As for V813		
Leucine (L820)	167.9	Phenylalanine (F)	203.4	
		Alanine (A)	91.5	
Glycine (G823)	66.4	Alanine (A)	91.5	
Alanine (A827)	91.5	Serine (S)	99.1	polar
		Valine (V)	141.7	
Valine (V830)	141.7	As for V813		
Glutamate (E834)	155.1	Glutamine (Q)	161.1	polar
		Aspartate (D)	124.5	like glutamate, charged
		Asparagine (N)	135.2	polar

Average volume values obtained from Table 2 in Richards (1977). Most side chains in the VVLGAVE face, except for glycine (G823) which has no side chain and glutamate (E834) which is charged, are non-polar. For substitutions, we generally selected amino acids whose side chains retained the chemical properties of the native side chain but had either a smaller or larger volume.

Table S2. **Single-channel properties of wild-type GluN1/GluN2A or tryptophan-substituted GluN1 or GluN2A NMDARs where whole-cell currents were significantly potentiated**

Construct	Total events (# of patches)	*i*	eq. P_o	MCT	MOT
		pA		*ms*	*ms*
N1/N2A	1,531,680 (10)	−7.2 ± 0.1	0.69 ± 0.04	2.3 ± 0.2	5.5 ± 0.5
N1(L819W)	73,124 (4)	−6.8 ± 0.3	0.80 ± 0.10	2.7 ± 1.3	11.3 ± 1.8*
N2A(M823W)	18,280 (4)	−6.7 ± 0.1	0.22 ± 0.04*	56.3 ± 7.7*	15.2 ± 2.5*

Values shown are mean ± SEM for single-channel current amplitude (*i*), equilibrium open probability (P_o), MCT, and MOT. Single-channel currents were recorded and analyzed as in Table 2. Number of patches is in parenthesis to the right of total events. Asterisks indicate values significantly different from wild type ($P < 0.05$, *t* test; see Materials and methods). The two tryptophan-substituted constructs, GluN1(L819W) and GluN2A(M823W), showed significant current potentiation of whole-cell current amplitudes (Fig. 3 B). We characterized fluorescence changes for these constructs (raw data not shown): 0.61 ± 0.02, $n = 15$ [GluN1(L819W)/GluN2A] and 0.49 ± 0.03, $n = 15$ [GluN1/GluN2A(M823W)]. These values were indistinguishable from their respective wild type, suggesting that increased current amplitudes were not caused by greater surface expression, though we cannot rule out some sort of bias in cell selection (see Materials and methods). In terms of single-channel activity, GluN1(L819W)/GluN2A showed behavior indistinguishable from wild type, whereas GluN1/GluN2A(M823W) showed significantly reduced eq. P_o (this table). The only common feature between these constructs was that both significantly increased MOT, which might in some way impact peak currents. In any case, the impact of these intermediate positions in the M4 on current potentiation is ambiguous. Though changes in gating, most notably an increase in MOT, may contribute to increased current amplitudes, we do not explore this issue further here.

REFERENCE

Richards, F.M. 1977. Areas, volumes, packing and protein structure. *Annu. Rev. Biophys. Bioeng.* 6:151–176. http://dx.doi.org/10.1146/annurev.bb.06.060177.001055